ภาคผนวก

(APPENDIX)

Available online at www.sciencedirect.com
ScienceDirect
ELSEVIER
Mechanical Systems and Signal Processing 21 (2007) 1174–1187
Mechanical Systems and Signal Processing
www.elsevier.com/locate/jnlabr/ymssp

Vibration response and harmonic wave propagation of ultrasonic arc drivers

Pruittikorn Smithmaitrie[a,*], J.G. DeHaven[b], K. Higuchi[c], H.S. Tzou[b]

[a]*Department of Mechanical Engineering, Faculty of Engineering, Prince of Songkla University, Hatyai, Songkla 90112, Thailand*
[b]*Department of Mechanical Engineering, StrucTronics Lab, University of Kentucky, Lexington, KY 40506-0503, USA*
[c]*Institute of Space and Astronautical Science, Kanagawa, Japan*

Received 28 June 2005; accepted 6 August 2005
Available online 26 September 2005

Abstract

A piezoelectric curvilinear arc driver designed for an ultrasonic curvilinear motor is evaluated in this study. A design of piezoelectric curvilinear arc driver is proposed and its governing equations, vibration behaviour and wave propagation are investigated. Then, analysis of forced vibration response or driving characteristics to harmonic excitations in the modal domain is conducted. Finite element modelling and analysis of the arc driver are also discussed. Analytical results of free vibration characteristics are compared favourably with the finite element results. Harmonic analyses of the three finite element models reveal changes of dynamic behaviours of three models and also imply operating frequencies with a significant travelling wave component. Parametric study of mathematical and finite element simulation results suggests that stable travelling waves can be generated to drive a rotor on the proposed curvilinear arc motor system.

Keywords: Finite element analysis; Piezoelectric actuator; Ultrasonic motor; Curvilinear motor

1. Introduction

Ultrasonic motors have been continuously developed and tested over a decade and most of ultrasonic vibration actuators are based on piezoelectric or electrostrictive materials bonded with elastic motor structures designed for either linear or rotary motions [1–3]. An ultrasonic motor system usually consists of a stator and a rotor and the travelling wave(s) generated at the stator driving the rotor is a key design parameter governing the overall motor performance. (Note that the travelling wave is also often referred as the propagating wave.) In this research, a curvilinear arc driver (stator) of an ultrasonic curvilinear arc motor illustrated in Fig. 1 is studied. The circular arc stator drives and guides a rotor along the arc to any specific angular position on the arc surface. Electro-dynamics, vibration characteristics and mechanical response of the designed curvilinear arc stator are investigated in this study.

*Corresponding author. Tel.:/fax: +66 74 212893.
E-mail address: spruitti@me.psu.ac.th (P. Smithmaitrie).

0888-3270/$ - see front matter © 2005 Elsevier Ltd. All rights reserved.
doi:10.1016/j.ymssp.2005.08.006

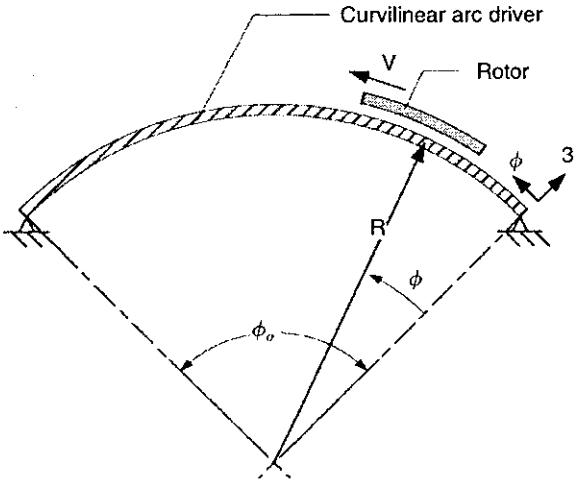

Fig. 1. Schematic diagram of the curvilinear arc driver/rotor.

Unlike vibrations in piezoelectric circular disk ultrasonic motors [1,2], boundary conditions of the circular arc reflect the waves when those generated waves reach the boundaries. This may generate undesirable standing waves interferencing the motor performance. There are techniques to generate travelling waves in finite length mediums. One technique is to use two actuators with one vibrator at one end to generate vibrations and one absorber at the other end to absorb those vibrations [4]. This technique generates only one-way travelling wave. Another technique is to use two vibrators at the opposite ends to generate travelling waves by superposing two standing waves with different phases [5]. This technique is capable of generating either forward or backward travelling wave by the paired vibrators operating in appropriate phases. The other technique is to use the piezoelectric patches bonded with an elastic medium producing travelling waves by superposing two standing waves. The pattern of piezoelectric patches is designed so that they can generate two sinusoidal waveforms at different time and location phases [2,6]. External vibrators are no longer needed in this set-up, since the waves are generated by bonded patches. This motor construction is relatively simple and flexible. However, wave reflection at the boundaries is prohibited, because this can interfere and distort the pattern of travelling waves. In practice, damping materials are attached to the boundaries to prevent the wave reflection. Ultrasonic motors made of finite length medium (e.g. plates and beams) laminated with piezoelectric have been reported [6–8], but those are designed for linear translational motions. Piezoelectric circular arc structures were also studied in vibration control applications [9–11]. Analytical evaluation of micro-actuations of piezoelectric actuator patches bonded on a curvilinear arc stator has been recently reported [12]. In this study, a design of piezoelectric curvilinear arc stator/motor is proposed and its governing equations, free-vibration characteristics, harmonic responses, and travelling waves are presented. Analytical solutions are compared with finite element (FE) results and the arc stator's driving capabilities and characteristics are evaluated.

2. Design and modelling of circular arc drivers

A stator driving mechanism consists of an elastic circular arc bonded with piezoelectric patches coordinated as a vibration actuator generating travelling waves driving a rotor in an ultrasonic motor system. Fig. 2 illustrates a piezoelectric actuator pattern design that produces a progressive in-plane flexural wave at the $k = 9$ mode shape. Design principle of the piezoelectric pattern was discussed [2,6] and analysis of actuator location and size was recently reported [12]. The length of one actuator patch is $\lambda/2$, where λ is the wavelength. Two groups of the actuators (top and bottom sets) are placed a quarter wavelength ($\lambda/4$) offset on the stator. The top and bottom groups are excited by a pair of electrical signals $A\cos(\omega t)$ and $A\sin(\omega t)$ respectively, where A is the amplitude and ω is the driving frequency. For a finite length medium, attenuation of the

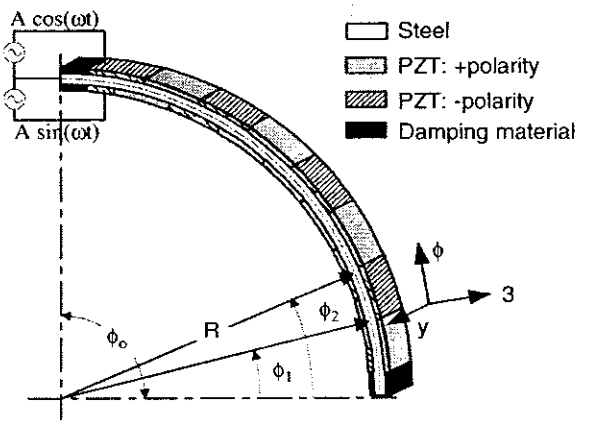

Fig. 2. The construction of piezoelectric circular arc driver.

travelling wave at the boundaries is crucial to form a stable travelling wave [6]. Accordingly, a damping segment to prevent the wave reflection is added between the rigid support and the piezoelectric actuator segment to maintain a stable travelling wave. In this design, a $\lambda/4$-length damping material is attached at the boundaries to prevent the wave reflection.

It is assumed that the segmented piezoelectric actuators are perfectly bonded with the elastic arc. An arbitrary segmented piezoelectric actuator patch is defined from ϕ_1 to ϕ_2 in the ϕ-direction and from y_1 to y_2 in the y-direction on the elastic arc (Fig. 2). Influence of the actuator mass on the overall system dynamics is neglected when defining the mathematical model of the system. However, the piezoelectric actuator-induced control force $N^c_{\phi\phi}$ and moment $M^c_{\phi\phi}$ are added to the governing equations of the circular arc and the equations of motion becomes [12]

$$\frac{\partial(N_{\phi\phi} - N^c_{\phi\phi})}{\partial\phi} + Q_{\phi 3} + Rq_\phi = R\rho h\frac{\partial^2 u_\phi}{\partial t^2}, \tag{1}$$

$$\frac{\partial Q_{\phi 3}}{\partial\phi} - \left(N_{\phi\phi} - N^c_{\phi\phi}\right) + Rq_3 = R\rho h\frac{\partial^2 u_3}{\partial t^2} \tag{2}$$

and

$$Q_{\phi 3} = \frac{1}{R}\frac{\partial\left(M_{\phi\phi} - M^c_{\phi\phi}\right)}{\partial\phi}, \tag{3}$$

where $N_{\phi\phi}$ is the elastic membrane force, $M_{\phi\phi}$ is the bending moment, $Q_{\phi 3}$ denotes the transverse shear stress resultant, q_i is the external excitation, ρ is the mass density, h is the arc thickness, and u_i is the displacement in the i-direction. Note that q_i can also be discrete or distributed control forces. Free vibration behaviours are analysed next, followed by actuation forces/moments and harmonic forced vibration analysis.

3. Free vibration and natural modes

It is assumed that the arc stator of the ultrasonic motor has simply supported boundary ends and its dominating vibration modes are (1) the circumferential modes $U_{\phi k}$ and (2) the transverse modes U_{3k}. Even and

odd natural mode shapes and their natural frequencies f_k are, respectively, defined as [12–14]

(1) *Even Modes*: $k = 2,4,6,\ldots$

$$f_k = \frac{k^2\pi^2}{2\pi(R\phi_0)^2}\left[\frac{\left\{1-\left(\frac{\phi_0}{k\pi}\right)^2\right\}^2}{1+3\left(\frac{\phi_0}{k\pi}\right)^2}\right]^{1/2}\sqrt{\frac{YI}{\rho hb}} \quad \text{for } k = 2,4,6,\ldots, \tag{4}$$

$$U_{\phi k} = \frac{\phi_0}{k\pi}\left[1-\cos\left(\frac{k\pi\phi}{\phi_0}\right)\right],$$

$$U_{3k} = -\sin\left(\frac{k\pi\phi}{\phi_0}\right). \quad \text{for } k = 2,4,6,\ldots. \tag{5,6}$$

(2) *Odd Modes*: $k = 3,5,7,\ldots$

$$f_k = \frac{k^2\pi^2}{2\pi(R\phi_0)^2}\left[\frac{\left\{1-\left(\frac{\phi_0}{k\pi}\right)^2\right\}^2}{1+\frac{1}{k^2}+2\left(\frac{\phi_0}{k\pi}\right)^2}\right]^{1/2}\sqrt{\frac{YI}{\rho hb}} \quad \text{for } k = 3,5,7,\ldots, \tag{7}$$

$$U_{\phi k} = -\frac{\phi_0}{k\pi}\left[\cos\left(\frac{k\pi\phi}{\phi_0}\right)-\frac{1}{\pi^3}\cos\left(\frac{\pi\phi}{\phi_0}\right)\right],$$

$$U_{3k} = -\sin\left(\frac{k\pi\phi}{\phi_0}\right)+\frac{1}{k}\sin\left(\frac{\pi\phi}{\phi_0}\right), \quad \text{for } k = 3,5,7,\ldots, \tag{8,9}$$

where k is the mode (or wave) number, f_k is the natural frequency in (Hz), Y is the modulus of elasticity, I is the area moment of inertia, ρ is the mass density, h is the thickness of the arc, b is the width of the arc, $U_{\phi k}$, U_{3k} are the kth mode shapes, respectively, corresponding to the ϕ- and 3-directions; ϕ defines the angular position on the arc; and ϕ_0 is the curvature angle of the arc. Examining the mode shape equations (Eqs. (5)–(6) and (8)–(9)) suggest that the transverse flexural mode dominates and the in-plane membrane mode diminishes at the high modes since the mode number appears on the denominator.

4. Actuation forces and moments

In this section, actuation forces and moments of a generic piezoelectric actuator laminated on a circular arc is discussed. The circular arc driver is bonded with a piezoelectric actuator patch defined from ϕ_1 to ϕ_2 in the angular position and has the same width as the arc stator b as illustrated in Fig. 3. It is assumed that the radius of curvature of the actuator patch is $(R+h/2+h^a/2)\approx R$, where h is the stator thickness and h^a is the actuator thickness. Thus, the effective actuator area S^e can be approximated as $Rb(\phi_2-\phi_1)$.

It is assumed that only a transverse voltage ϕ^a is applied. If the electrode resistance is neglected, the voltage across the piezoelectric actuator patch is constant. Thus, an actuator voltage $\phi^a(y,\phi,t)$ applied to the distributed piezoelectric actuator patch is

$$\phi^a(y,\phi,t) = \phi^a(t)\left[u_s(y-y_1)-u_s(y-y_2)\right]\left[u_s(\phi-\phi_1)-u_s(\phi-\phi_2)\right], \tag{10}$$

where u_s represents a unit step function, $u_s(\phi-\phi_i)=1$ when $\phi\geqslant\phi_i$, and $=0$ when $\phi<\phi_i$. The spatial derivatives are

$$\frac{\partial}{\partial\phi}\phi^a(y,\phi,t) = \phi^a(t)\left[u_s(y-y_1)-u_s(y-y_2)\right]\left[\delta(\phi-\phi_1)-\delta(\phi-\phi_2)\right], \tag{11}$$

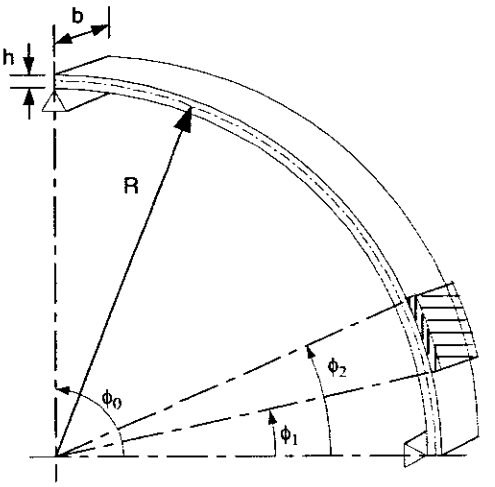

Fig. 3. A piezoelectric laminated circular arc.

where $\delta(\cdot)$ is the Dirac delta function: $\delta(\phi-\phi_i)=1$ when $\phi=\phi_i$, and 0 when $\phi\neq\phi_i$. Then, the actuation force $N^c_{\phi\phi}$ and actuation moment $M^c_{\phi\phi}$ in the ϕ-direction induced by the piezoelectric actuator patch can be defined as

$$N^c_{\phi\phi}=Y_p d_{31}\phi^a\left[u_s(y-y_1)-u_s(y-y_2)\right]\left[u_s(\phi-\phi_1)-u_s(\phi-\phi_2)\right], \tag{12}$$

$$M^c_{\phi\phi}=r^a Y_p d_{31}\phi^a\left[u_s(y-y_1)-u_s(y-y_2)\right]\left[u_s(\phi-\phi_1)-u_s(\phi-\phi_2)\right], \tag{13}$$

where Y_p is the actuator elastic modulus, d_{31} is the piezoelectric strain constant, r^a is the effective moment arm (distance from the neutral surface to the mid-plane of the actuator patch).

5. Harmonic excitation and response

The modal expansion method is used to evaluate forced vibration behaviour and harmonic response of the arc stator. It is assumed that the excitation force is independent of the motion of the structure and the amount of participation of each mode in the total dynamic response is defined by the modal participation factor [15]. Thus, the total response of the arc, i.e. $u_i(\phi,t)$, can be written as

$$u_i(\phi,t)=\sum_{k=2}^{\infty}\eta_k(t)U_{ik}(\phi), \tag{14}$$

where $i=\phi,3$; $\eta_k(t)$ is the modal participation factor and $U_{ik}(\phi)$ is the mode shape function in the i-direction. Using Eq. (14), integrating over the arc surface and imposing modal orthogonality [15], one can derive the kth modal equation of the circular arc as

$$\ddot{\eta}_k+2\zeta_k\omega_k\dot{\eta}_k+\omega_k^2\eta_k=\hat{F}_k^m(t)+\hat{F}_k^c(t)\equiv\hat{F}_k(t), \tag{15}$$

where the modal damping ratio $\zeta_k=c/2\rho h\omega_k$ and c is the damping factor usually experimentally estimated, ω_k is the kth mode natural frequency; $\hat{F}_k^m(t)$ is the mechanical excitation, $\hat{F}_k^c(t)$ is the electrical control excitation, $\hat{F}_k(t)$ is the total modal force. In this case, it is assumed that the mechanical excitation is neglected thus the excitation $\hat{F}_k(t)$ is the only electrical actuation input used to generate driving waves. The curvilinear arc driver is excited by harmonic electrical excitations as shown in Fig. 2. Accordingly, the steady-state response to harmonic excitation can be determined as follows:

The excitation force $\hat{F}_k(t)$ in Eq. (15) can be separated into a harmonic excitation part $e^{j\omega t}$ and a spatial part $\hat{F}_k'$, i.e.,

$$\hat{F}_k(t)=\hat{F}_k'e^{j\omega t}, \tag{16}$$

where

$$\hat{F}'_k = \frac{1}{\rho h N_k} \int_y \int_\phi \left\{ \sum_i L_i^{c'}(\phi^a) U_{ik} \right\} A_1 A_2 \, \mathrm{d}\phi \, \mathrm{d}y \tag{17}$$

and ω is the excitation frequency, $L_i^{c'}(\phi^a)$ is the electrical Love's operator derived from the converse piezoelectric effect and it is defined as a function of spatial coordinates only [16]. The modal participation equation further becomes

$$\ddot{\eta}_k + 2\zeta_k \omega_k \dot{\eta}_k + \omega_k^2 \eta_k = \hat{F}'_k e^{j\omega t}. \tag{18}$$

For a harmonic excitation, the steady-state response of modal participation factor $\eta_k(t)$ is also a harmonic function.

$$\eta_k(t) = \Lambda_k e^{j(\omega t - \phi_k)}. \tag{19}$$

Substituting Eq. (19) into Eq. (18) and rearranging gives

$$\Lambda_k e^{-j\phi_k} = \frac{\hat{F}'_k}{(\omega_k^2 - \omega^2) + 2j\zeta_k \omega_k \omega}. \tag{20}$$

The magnitude Λ_k and phase lag ϕ_k of the harmonic response are

$$\Lambda_k = \frac{\hat{F}'_k}{\omega_k^2 \sqrt{\left[(1 - (\omega/\omega_k)^2)\right]^2 + 4\zeta_k^2 (\omega/\omega_k)^2}}, \tag{21}$$

$$\phi_k = \tan^{-1}\left[\frac{2\zeta_k (\omega/\omega_k)}{1 - (\omega/\omega_k)^2} \right]. \tag{22}$$

Substituting Love's operators into Eq. (17) gives

$$\hat{F}'_k = \frac{1}{\rho h N_k} \int_y \int_\phi \left\{ \left(-\frac{1}{R} \left(\frac{\partial N^c_{\phi\phi}}{\partial \phi} + \frac{1}{R} \frac{\partial M^c_{\phi\phi}}{\partial \phi} \right) \right) U_{\phi k} + \left(-\frac{1}{R} \left(\frac{1}{R} \frac{\partial^2 M^c_{\phi\phi}}{\partial \phi^2} - N^c_{\phi\phi} \right) \right) U_{3k} \right\} A_1 A_2 \, \mathrm{d}\phi \, \mathrm{d}y. \tag{23}$$

Eq. (23) shows that the modal control force consists of four control force components. There are (1) the membrane component $\hat{T}_{k\_U\phi,\mathrm{mem}}$ induced by $U_{\phi k}$ (2) the membrane component $\hat{T}_{k\_U_3,\mathrm{mem}}$ induced by U_{3k} (3) the bending component induced $\hat{T}_{k\_U_\phi,\mathrm{bend}}$ by $U_{\phi k}$ and (4) the bending component induced $\hat{T}_{k\_U_3,\mathrm{bend}}$ by U_{3k}. Hence, the modal control force can be expressed in terms of control membrane and bending components as follows:

$$\hat{F}'_k = \hat{T}_{k\_U\phi,\mathrm{mem}} + \hat{T}_{k\_U_3,\mathrm{mem}} + \hat{T}_{k\_U_\phi,\mathrm{bend}} + \hat{T}_{k\_U_3,\mathrm{bend}} \tag{24}$$

and

$$\hat{T}_{k\_U_\phi,\mathrm{mem}} = \frac{Y_p d_{31} \phi^a b}{\rho h N_k} (U_{\phi_2 k} - U_{\phi_1 k}), \tag{25}$$

$$\hat{T}_{k\_U_3,\mathrm{mem}} = \frac{Y_p d_{31} \phi^a b}{\rho h N_k} \int_{\phi_1}^{\phi_2} U_{3k} \, \mathrm{d}\phi, \tag{26}$$

$$\hat{T}_{k\_U_\phi,\mathrm{bend}} = \frac{r^a Y_p d_{31} \phi^a b}{R \rho h N_k} (U_{\phi_2 k} - U_{\phi_1 k}), \tag{27}$$

$$\hat{T}_{k\_U_3,\text{bend}} = \frac{r^a Y_p d_{31} \phi^a b}{R\rho h N_k} \left(\left. \frac{\partial U_{3k}}{\partial \phi} \right|_{\phi=\phi_1} - \left. \frac{\partial U_{3k}}{\partial \phi} \right|_{\phi=\phi_2} \right), \tag{28}$$

where Y_p is the actuator elastic modulus, d_{31} is the piezoelectric strain constant, r^a is the effective moment arm (a distance from arc's neutral surface to the mid-plane of the actuator patch) and ϕ^a is a transverse applied voltage. To analyse the system dynamic responses, the mechanical properties of piezoelectric arc structure are considered based on elastic properties of the lamina. By the rule of mixtures, density of the structure is

$$\rho_c = v_{\text{pzt}} \rho_{\text{pzt}} + v_{\text{stator}} \rho_{\text{stator}}. \tag{29}$$

Young's modulus in transverse direction is estimated as

$$Y_c = \frac{Y_{\text{stator}} Y_p}{(v_p Y_{\text{stator}} + v_{\text{stator}} Y_p)}, \tag{30}$$

where v_p is the volume fraction of piezoelectric material, v_{stator} is the volume fractions of the stator material and Y_{stator} is the Young's modulus of the stator material [17,18]. It is assumed that effect of damping materials added to boundaries can be neglected in the effective density, Eq. (29), and Young's modulus, Eq. (30), of the structure. The harmonic steady-state force response is analysed. Based on the principle of superposition, the total forced response of the piezoelectric circular arc can be determined by superposing the responses induced by respective actuator patches. In order to validate the analytical solutions, the piezoelectric circular arc stator is also modelled and analysed with a FE code ANSYS. FE modelling is discussed next.

6. Finite element analysis

A FE software (ANSYS) is used to model the piezoelectric curvilinear arc driver and to evaluate the system responses in case studies. In this FE analysis, influence of piezoelectric actuator to the system dynamics is taken into consideration. The stator system model consists of a steel circular arc (i.e. the stator structure), piezoelectric actuator patches and damping materials (Fig. 2). It is assumed that there is no in-plane deflection in the y-direction. Hence, the system is simplified to a 2D problem. In ANSYS, PLANE13 element type is used to simulate the coupled-field (electromechanical) effect of piezoelectric material. The elements and nodal coordinates of the FE model are rotated parallel to local cylindrical coordinate.

There are two types of boundary conditions evaluated in ANSYS analyses. One is the simply support boundary condition. However, in practice, it is difficult to implement ideal simply support boundary conditions. Hence, a second type boundary condition, i.e. the modified-simply support boundary condition, is considered to mimic the experimental boundary condition. The modified-simply support boundary condition consists of (1) nodal displacements of boundary nodes at $\phi = 0$ and $\pi/2$ in the ϕ-direction are zero and (2) nodal displacements of stator's mid-span at $\phi = 0$ and $\pi/2$ in the 3-direction are zero. Furthermore, the sinusoidal electrical excitations with amplitude of 10 V are applied on the surface nodes of piezoelectric actuators. Dimensions of the circular arc are arc radius $R = 60$ mm, arc width $b = 9$ mm, arc thickness $h = 1$ mm, arc angle $\phi_0 = \pi/2$, and piezoelectric lead zirconate-titanate (PZT-4) actuator thickness $h^a = 0.5$ mm. Other material properties of the circular arc stator, piezoelectric actuator and damping material are summarised in Table 1.

7. Evaluation of stator characteristics

Dynamic behaviour and harmonic characteristics of the ultrasonic arc stator system are evaluated using the analytical and FE techniques in this section. Natural frequencies are evaluated first, followed by forced harmonic responses and driving characteristics at various excitation frequencies to determine the operating frequencies generating perfect travelling waves.

Table 1
Material Properties

	Lead–Zirconate–Titanate PZT-4 actuator[a]	Steel circular arc	Silicon rubber damping material	Unit
Young's modulus	80 (Yp)	210 (Y_{stator})	4.2×10^{-3} (Y_d)	GPa
Density	7550 (ρ_p)	7860 (ρ_{stator})	1510 (ρ_d)	kg/m^3
Poisson's ratio	0.34 (μ_p)	0.27 (μ_{stator})	0.45 (μ_d)	
Damping coefficient	—	—	0.002	
Piezoelectric constant				
d_{31}	-1.2×10^{-10}	—	—	m/V
e_{33}	15.1	—	—	C/m^2
e_{31}	−5.2	—	—	C/m^2
e_{15}	12.7	—	—	C/m^2
Permittivity	1.15×10^{-8} (ε_{33})	—	—	F/m

[a]Ref. [19].

Table 2
The in-plane natural frequencies of the arc stator

Mode (k)	Natural Frequencies (Hz)				
	Analytical (Without PZT)	ANSYS (Without PZT)	Analytical (With PZT)	ANSYS (With PZT)	ANSYS (PZT/ modified support)
2	908	944	1362.4	1350	1819
3	2138	2222	3207.3	3119	3688
4	4062	4243	6094.4	5868	6984
5	6343	6616	9517.5	8709	9679[a] and 12 322[a]
6	9337	9796	14 009	13 106	15 182
7	12 671	12 701[a] and 14 524[a]	19 012	18 121	20 717
8	16 724	17 657	25 093	22 901	24 637
9	21 113	22 627	31 678	29 827	33 089
10	26 223	27 791	39 345	37 140	40 563
11	31 666	34 132	47 513	44 863	47 318

[a]antisymmetric mode about midspan.

7.1. Natural frequencies

From the given dimensions and material properties (Table 1) of the ultrasonic stator system, the in-plane flexural natural frequencies (mode $k = 2,3,4 \ldots 11$) of the models with and without piezoelectric layers are, respectively, calculated and compared (Table 2).

Comparing the analytical data (the 1st column) and the FE results (the 2nd column) of the circular arc without piezoelectric actuators shows that the natural frequencies are compared well, i.e. about 4% difference at low modes and about 7.8% difference at high modes. Then, the piezoelectric actuator patches are integrated into the stator system and the analytical natural frequencies (the 3rd column) are still comparable with the ANSYS results (the 4th column). The results show that the natural frequencies increase when integrating piezoelectric actuators into the stator system, because piezoelectric actuators increase the system stiffness. The last column shows that the modified simply support also increases the natural frequencies due to the increased system stiffness as well. Note that the motor operating frequency should be in ultrasonic range (above 20 kHz) in order to avoid audible noise. Thus, the 9th mode is selected to be the operating mode and the PZT patch pattern is designed to generated travelling wave corresponding to the operating mode (Fig. 2). Curvilinear arc stator responses to harmonic electrical excitations are studied next.

7.2. Forced vibration responses

The piezoelectric circular arc stator is considered as a composite lamina. It is assumed that the system is undamped and boundary condition is simply support. The top and bottom groups of piezoelectric actuators are excited by electrical signals $10\cos(\omega t)$ and $10\sin(\omega t)$, respectively. Analytical data of the simply supported stator model indicate that the travelling waves can be generated within narrow bands of excitation frequencies, due to specified actuator design patterns. Figs. 4 and 5 illustrate the wave propagations at excitation frequencies of 18 102 and 50 000 Hz respectively. These results suggest that the propagating waves well occur at approximately 18 and 50 kHz. Comparing these two operating frequencies indicates that the wave amplitude at the low operating frequency (18 102 Hz) is higher than that of the high operating frequency (50 000 Hz). But the number of wave crests at the high operating frequency is greater than that at the low operating frequency.

Sine sweep excitation, i.e. changing excitation frequencies, is used to examine the travelling and standing wave components in the total system response. Simulation results show that pure standing waves occur when the system is excited within narrow bands of the natural frequencies. Otherwise, the waves are combinations of travelling and standing waves. It appears that the amplitude of the travelling waves is not consistent along the arc length and the standing waves mostly occur near the boundaries. Effective travelling waves driving a rotor need consistent amplitudes along the arc length. However, in practice, the consistent-amplitude section is less than the arc length, since the waves have to dissipate at boundaries in order to avoid wave reflections. (Note that travelling waves of the arc stator are different from those of a full-revolution piezoelectric disk motor with free boundary conditions.) To select a suitable design, to maximise the consistency of wave amplitudes, and to decrease the wave reflection on the arc stator, damping materials are integrated into the system boundaries (Fig. 2). Accordingly, the boundary conditions need to be modified to mimic boundary conditions in practical implementation. Because of the limitation of analytical solution technique to deal with the modified boundary condition, a FE model is used to further evaluate the harmonic responses presented next.

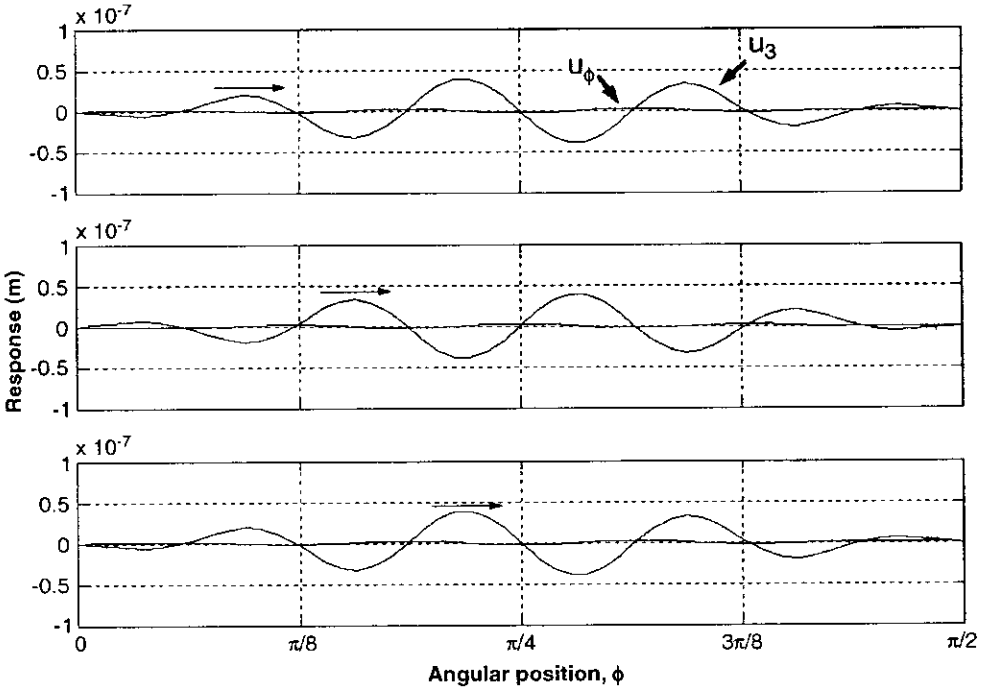

Fig. 4. The wave propagation on piezoelectric circular arc at 18 102 Hz.

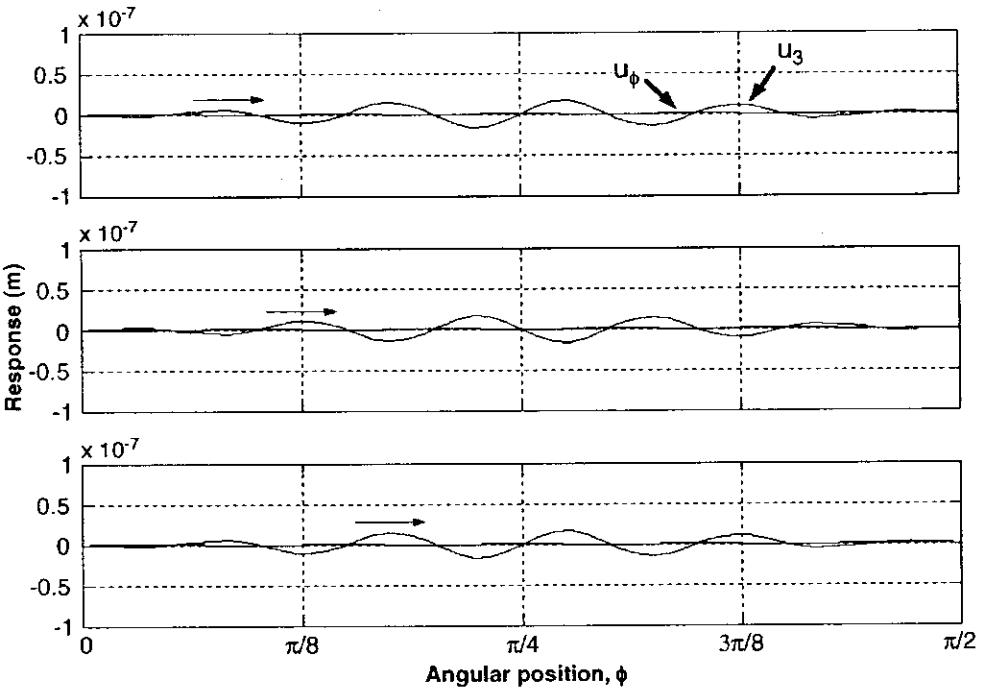

Fig. 5. The wave propagation on piezoelectric circular arc at 50 000 Hz.

7.3. Harmonic analysis of curvilinear arc stator

Three FE models of the arc stator i.e. (1) the simply supported boundary condition, (2) the modified simply supported boundary condition, and (3) the modified simply supported boundary condition with damping materials) are used to study the harmonic responses of the curvilinear arc stator subjected to the sinusoidal electrical excitations with amplitude of 10 V. The top group actuators are excited with $10\cos(\omega t)$ while the bottom ones are subjected to $10\sin(\omega t)$. The excitation frequency ω is varied from 0 to 60 000 Hz. Transverse displacement responses of the mid-span node at $\phi = \pi/4$ are obtained for the three FE models with various boundary conditions. Fig. 6 shows the frequency response of the arc stator system with simply support boundary condition; Fig. 7 shows the response of the structure without the damping material, but with the modified simply supported boundary conditions; and Fig. 8 illustrates the response of the structure with damping materials and modified boundary conditions. Comparing Figs. 6 and 7 indicate that the resonance and antiresonance frequencies of the arc stator system increase when boundary conditions are modified. This implies the structure becomes stiffer. Comparing Figs. 7 and 8 suggests that the resonance and antiresonance frequencies do not change, but their amplitudes decrease after the damping materials are added to the system.

The harmonic analysis results (Figs. 6–8) suggest that the amplitudes of the mid-span node are high when the system is excited in the neighbourhood of the natural frequencies and the present actuator design pattern does not excite all natural modes [12]. However, these harmonic frequency responses do not reveal what frequency ranges that yield the travelling waves. Accordingly, wave propagation characteristics in time-domain are analysed next.

7.4. Wave propagation of curvilinear arc stator

To evaluate the wave propagation (or travelling wave) characteristics, the third FE model – the candidate prototype model (i.e. with modified B.Cs and damping) is analysed. Examining the time-history responses at various excitation frequencies suggests that pure standing waves occur when the system is excited within a narrow band of the natural frequencies and pure travelling waves occur at excitation frequencies

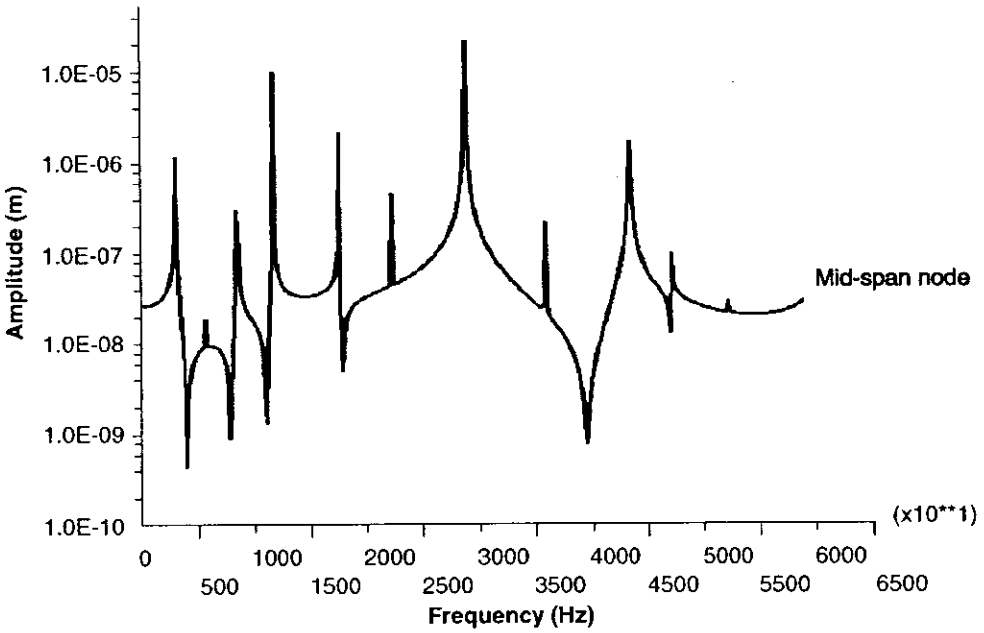

Fig. 6. Harmonic response of the simply supported arc stator.

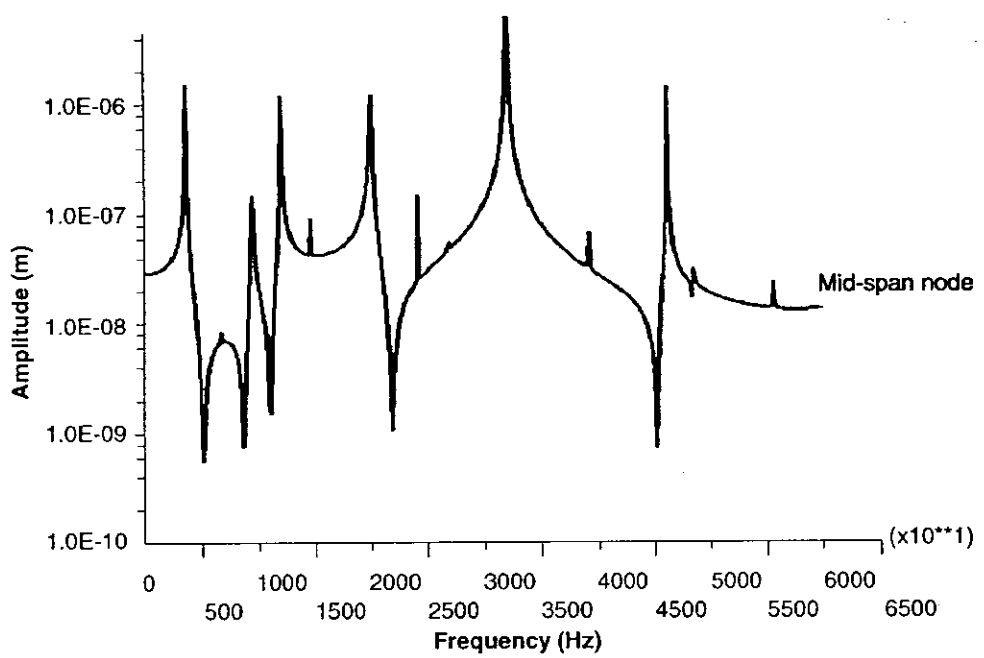

Fig. 7. Harmonic response of the modified simply supported arc stator without damping material.

approximately 18 and 47 kHz for the stator with damped boundary condition, as illustrated in Figs. 9 and 10. Otherwise, the responses are combinations of standing and travelling waves.

Referring to the harmonic response in Fig. 8, 18 and 47 kHz are in the range of antiresonance frequencies. This implies that the pure travelling waves occur at antiresonance frequencies. Investigating the simulation results also suggests that the added damping materials improve the travelling wave especially at the high

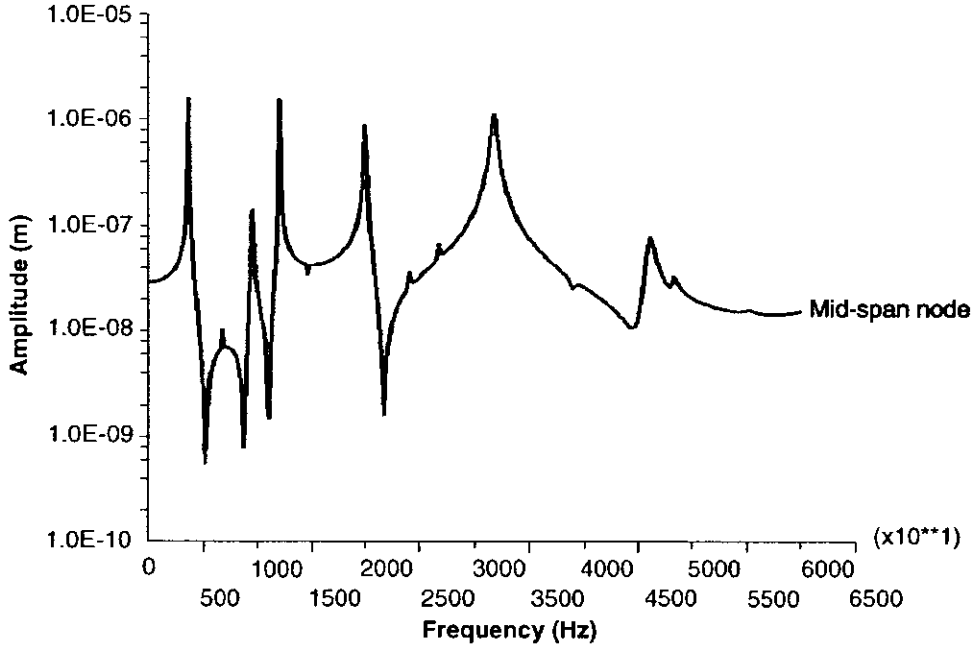

Fig. 8. Harmonic response of the modified simply supported arc stator with damping materials.

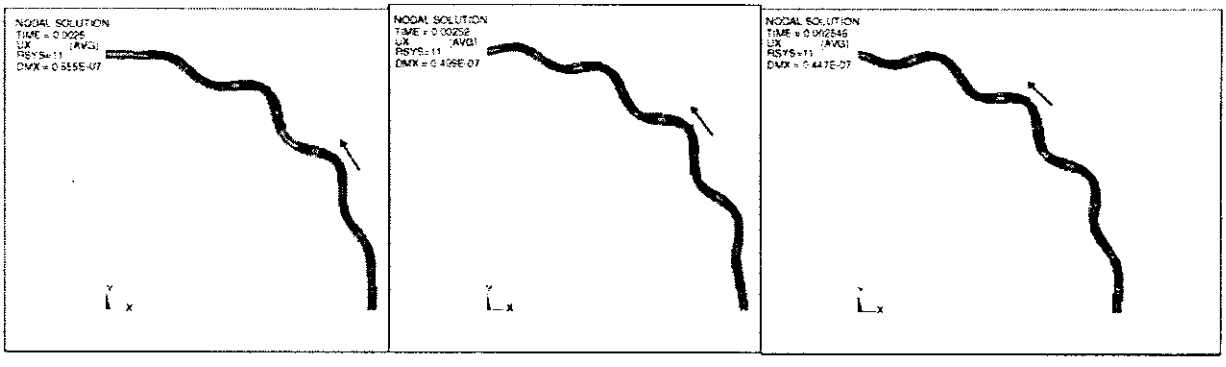

Fig. 9. Response of the stator in time domain at 18 102 Hz by ANSYS.

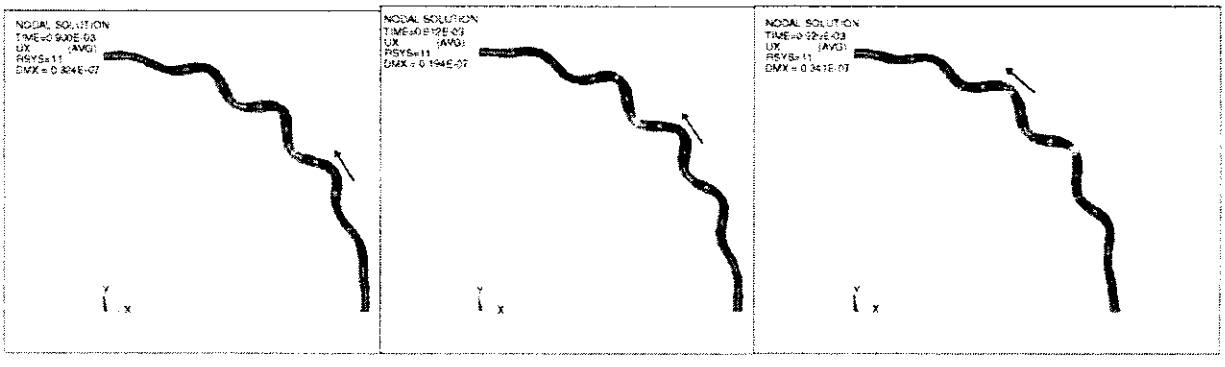

Fig. 10. Response of the stator in time domain at 47 200 Hz by ANSYS.

operating frequencies in the selected design. To further evaluate the operating frequencies, time-domain simulations of the analytical solutions of the simply supported (the 1st) model are also carried out. The inferred operating frequencies are, respectively, 18 and 50 kHz (Figs. 4 and 5) and these are very close to the FE predictions. Although the models are slightly different, these data provide a good estimation of the selected stator design.

8. Conclusions

The objective of this study is to evaluate dynamic characteristics and curvilinear wave generation of an ultrasonic arc stator designed as a key driver component in an ultrasonic curvilinear motor. Based on the proposed actuator pattern and structural design, its system governing equations, free-vibration behaviour, harmonic responses and wave (i.e. standing and travelling) characteristics were discussed in this study. Analytical solutions were compared with finite element (FE) (ANSYS) simulation results. Furthermore, dynamic effects and wave characteristics contributed by various boundary conditions, i.e. with and without damping materials, were studied based on FE simulations of three FE models. Both analytical data and ANSYS simulation results suggest the same trend that pure standing waves occur when the system is excited within narrow bands of the resonance frequencies. The analytical result of the model with the simply supported boundary condition yields the travelling waves at the operating frequencies approximately 18 and 50 kHz. The FE analysis of the model with the modified simply supported boundary condition and damping materials gives the operating frequencies at approximately 18 and 47 kHz. Although the models are slightly different, these data provide a good estimation of the selected stator design. The amplitude of the travelling wave at the low operating frequency is greater than that at the high operating frequency. At other excitation frequencies, the waves are combinations of standing and travelling waves. In summary, a design of piezoelectric curvilinear arc driver (stator) is proposed and simulated to determine operating frequencies by both analytical and FE methods. Analysis data suggests that stable travelling waves can be generated in the finite length circular arc by bonded piezoelectric actuator segments. Design and analysis methodology presented in this paper also serves an effective procedure to predict the curvilinear motion and dynamic characteristic of ultrasonic motor designs and applications. Prototyping of the proposed design is underway and its testing and performance evaluation will be reported shortly.

Acknowledgements

This research is supported, in part, by a grant from the Thailand Research Fund (TRF) and Commission on Higher Education. This support is gratefully acknowledged.

References

[1] T. Sashida, T. Kenjo, An Introduction to Ultrasonic Motors, Clarendon Press, Oxford, NY, 1993.
[2] S. Ueha, Y. Tomikawa, M. Kurosawa, N. Nakamura, Ultrasonic motors: Theory and Application, Clarendon Press, Oxford, NY, 1993.
[3] K. Uchino, Piezoelectric Ultrasonic Motors: Overview, Smart Material and Structures 7 (1998) 273–285.
[4] M. Kuribayashi, S. Ueha, E. Mori, Excitation conditions of flexural traveling waves for a reversible ultrasonic linear motor, Journal of the Acoustical Society of America 77 (4) (1985) 1431–1435.
[5] K. Higuchi, A piezoelectric linear motor driven by superposing standing waves with phase difference, in: *AIAA/ASME/ASCE/AHS/ASC 36th Structures, Structural Dynamics and Materials Conference and AIAA/ASME Adaptive Structures Forum*, 1995, New Orleans, LA. 10–13 April, pp. 3296–3304.
[6] Y. Roh, S. Lee, W. Han, Design and fabrication of a new traveling wave-type ultrasonic linear motor, Sensors and Actuators 94 (2001) 205–210.
[7] Y. Tomikawa, T. Nishitsuka, T. Ogasawara, T. Takano, A paper or card forwarding device using a flat-type ultrasonic motor, Sensors and Materials 1 (6) (1989) 359–379.
[8] T. Kosawada, K. Suzuki, Y. Tomikawa, 1992, A card sending linear ultrasonic motor using multi-beam piezoelectric vibrators, in: J. Tani, T. Tagaki, (Eds.), *Electromagnetic Forces and Applications*, Proceeding of the Third International ISEM Symposium on the Application of Electromagnetic Forces, Sendai, Japan, 18–20 January 1991, Elsevier Science Publishers, New York, pp. 35–38.

[9] H.T. Banks, Y. Zhang, Computational method for a curved beam with piezoceramic patches, Journal of Intelligent Material System and Structures 8 (3) (1997) 260–278.
[10] V.R. Sonti, J.D. Jones, Curved piezoactuator model for active vibration control of cylindrical shells, AIAA Journal 34 (5) (1996) 1034–1040.
[11] H.R. Shih, Distributed vibration sensing and control of a piezoelectric laminated curved beam, Smart Materials and Structures 9 (6) (2000) 761–766.
[12] P. Smithmaitrie, H.S. Tzou, Electro-dynamics, micro-actuation and design of ultrasonic curvilinear arc stators, Journal of Sound and Vibration 284 (3–5) (2005) 635–650.
[13] R.D. Blevins, Formulas for Natural Frequency and Mode Shape, reprint ed, Krieger Publisher Company, Florida, 1995.
[14] A.S. Veletsos, W.J. Austin, C.A. Lopes Pereira, S.J. Wung, Free in-plane vibration of circular arches, *Journal of the Engineering Mechanics Division*, Proceeding of the American Society of Civil Engineers 98 (1972) 311–329.
[15] W. Soedel, Vibrations of Shells and Plates, Marcel Dekker, New York, 1981.
[16] H.S. Tzou, Piezoelectric Shells (Distributed Sensing and Control of Continua), Kluwer Academic Publishers, Boston/Dordrecht, 1993.
[17] I.M. Daniel, O. Ishai, Engineering Mechanics of Composite Material, Oxford University Press, New York, 1994.
[18] R.M. Jones, Mechanics of Composite Materials, Taylor & Francis, Pennsylvania, 1999.
[19] O.E. Mattiat, Ultrasonic Transducer Materials, Plenum Press, New York, 1971.